CEAS Aeronautical Journal
https://doi.org/10.1007/s13272-023-00659-w

ORIGINAL PAPER

Aerodynamic model adjustment for an accurate flight performance representation using a large operational flight data base

Christoph Deiler[1]

Received: 12 December 2022 / Revised: 2 March 2023 / Accepted: 28 March 2023

Abstract
A novel process to determine an aircraft performance model from operational flight data with limited a priori knowledge is developed. The given big data problem is solved by application of fundamental engineering knowledge and a specific data evaluation strategy. The resulting smart data approach is fundamentally different from existing deep learning methods to solve such big data problems. A given aerodynamic model is updated to represent the characteristics of an Airbus A320neo aircraft based on a given large database of operational flights. The updated aerodynamic model implementation for one specific flap/slat configuration is exemplarily compared to the information available from flight data and the results are discussed in terms of model quality.

Keywords Flight performance model · Big data · Operational flight data analysis · System identification

List of symbols

a_x, a_y, a_z	Body-fixed accelerations, m/s^2
$C_{(\cdot)}$	Aerodynamic coefficient
$C_{(\cdot),\mathrm{M}}$	Aerodynamic coefficient derived from flight data measurements
C_D	Drag coefficient
C_{D0}	Zero-lift drag coefficient
C_L	Lift coefficient
C_{L0}	Lift coefficient at $\alpha = 0°$
$c_1, \alpha^\star$	Separation point function parameters
D	Drag force, N
e	Oswald factor
T	Engine thrust force, N
g	Gravitational acceleration, m/s^2
i_{HT}	Horizontal stabilizer deflection, rad
k_1	Drag model parameter
L	Lift force, N
Ma	Mach number
N	Number of measurements
q	Pitch rate, rad/s
$\overline{q}$	Dynamic pressure, Pa
$r_{\mathrm{HT}}, r^\star_{\mathrm{HT}}$	Horizontal tail lever arms, m
S	Surface area, m^2
t	Time, s
V_{TAS}	True airspeed, m/s
x, x_a	Longitudinal direction coordinates, body-fixed and aerodynamic, m
$\hat{X}_0$	Non-dimensional location of the wing separation point
X, Y, Z	Body-fixed forces, N
$\boldsymbol{y}$	Simulated model output vector
Y	Side force, N
$\boldsymbol{z}$	Measurement vector
α	Angle of attack, rad
α_{dyn}	Dynamic angle of attack of the horizontal tail, rad
β	Angle of sideslip, rad
δ	Control input (deflection)
ϵ_{HT}	Downwash angle at the horizontal tail, rad
η	Elevator deflection, rad
$\boldsymbol{\theta}$	Parameter vector
ξ	Aileron deflection, rad
ATRA	Advanced technology research aircraft
CG	Center of gravity
E	Engine
HT	Horizontal tail
LG	Landing gear
SP	Spoiler
WB	Wing/body

✉ Christoph Deiler
christoph.deiler@dlr.de

[1] Institute of Flight Systems, DLR - German Aerospace Center, 38108 Braunschweig, Germany

Published online: 20 April 2023

1 Introduction

Aircraft operations are mainly driven by the aircraft's flight performance. Therefore, new developments always target better aerodynamic performance and propulsion system efficiency with less energy consumption in order to reduce the operational costs and environmental impact of each individual flight. Hence, the optimization of an aircraft's flight performance is key to sustainable future aviation. Europe's Flight Path 2050 [1] describes the vision of technologies and procedures available in the year 2050 that will allow a reduction of 75% of the CO_2 emissions and 90% of the NO_x emissions per passenger kilometer compared to the year 2000. In addition, the perceived noise emission of an aircraft in flight must be reduced by 65%.

Within a short-term perspective, the reduction of emissions and pollution can only be achieved by new technologies enabling today's modern aircraft to be even more environmentally friendly and allow a greener aviation. For the best possible reduction of emissions with current fleets, an optimization of aircraft operations is required using smart flight control strategies. One of these strategies is DLR's Low Noise Augmentation System (LNAS) [2, 3], which is able to optimize the aircraft's descend and approach by advising the pilots with optimized autopilot commands and configuration points. It has proven during flight tests that its application can save up to 25% of fuel and emissions for certain approach flight phases. In addition, measurements on ground revealed that a significant noise reduction could be obtained when using LNAS: with an overall reduction on ground along the approach path certain areas show a reduction up to 5 dB. But the system relies on a high-quality simulation model for aircraft flight performance evaluation which is used within the internal flight path analysis and optimization process.

There are several ways to obtain such simulation models which base on different sources of information about the distinct aircraft type. For example, the simulation model formulation could be based on published aerodynamic and engine data, e.g., from handbooks or aircraft manuals [4]. Unfortunately, aircraft manuals do normally not contain the engine thrust values but only engine state information, which makes it impossible to obtain engine thrust models without additional information. Moreover, accurate aerodynamic performance charts are normally not published. Furthermore, one could use high-fidelity aircraft and engine design models to obtain the necessary information for generating aircraft flight performance models. Such an approach is mainly used by aircraft manufacturers, because they have full insight in the aircraft design process. If available, ground test data and wind tunnel results can also be used to determine a propulsion system model, e.g., Ref. [5], but the corresponding information are also mostly limited to engine manufacturers. For aerodynamic models, wind tunnel data would reveal the required information, but these data are also mostly confidential and not available even for scientific use. Another way to obtain the required information and to determine flight performance models is the conduction of special flight test programs with an aircraft of the specific type and use flight data recordings to extract the information about the flight performance. But even with extensive and expensive flight test programs, additional a priori information on e.g., engine thrust might be necessary to develop reliable flight performance models.

A completely different fourth way is to only use flight data gathered during operational flights, which can be easily recorded daily. But without dedicated flight test procedures, this will pose a big data problem which has to be solved. Nevertheless, the desired information is inside this data base, and if the data base is large enough, the information can be extracted by application of proper methodologies and algorithms. Big data problems and artificial intelligence methods to solve these are omnipresent today. But to solve a certain big data problem with minimal effort, the simple application of e.g., deep learning with artificial neural networks is no smart solution as their training is very time consuming and the resulting black box models lack of any interpretability. A smarter way to solve a big data problem in engineering is to apply as much fundamental knowledge about the underlying system as possible. This way big data is converted to smart data and the initially posed problem can be solved with much simpler, faster and presumably more deterministic methods. For operational flight data, this means that engineering knowledge about aircraft flight mechanics is applied and the data analysis process is designed accordingly. Doing so, well-established model formulations can be used which further allow a direct interpretation of the resulting model, e.g., evaluation of lift-to-drag ratio. In this way, the big data analysis of operational data can directly help to reduce aircraft emissions and make aviation sustainable.

This paper presents a part of the work on solving the described big data problem in a smart and intelligent engineering way in order to reveal the flight performance, aerodynamics and engine thrust from operational flight data of three different Airbus A320neo (New Engine Option) aircraft. It is based on previous DLR research on the determination of flight performance variations within operational flight data [6, 7] and has a different focus than already established methods for flight performance monitoring and model determination, e.g., [8–11]. A dedicated process is developed in order to reduce the data size and necessary computational effort.

The paper is structured as follows giving information about:

(1) challenges in the determination of flight performance models from flight data with (very) limited a priori information and the smart approach used in this work in Sect. 2;
(2) the data base of operational flight data in Sect. 3;
(3) the aerodynamic model formulation in Sect. 4;
(4) the engine model determination in Sect. 5;
(5) the aerodynamic model update based on flight data together with a statistical evaluation on the model quality in Sect. 6.

A summary and conclusions on the overall results are given in Sect. 7.

2 Challenges in flight performance model determination

For this work, the information about the Airbus A320neo was very limited except for the operational flight data. The main goal of a reliable flight performance model is hard to achieve if no broad base of information about the vehicle is available. Nevertheless, the challenges can be overcome with reasonable, engineering knowledge-based assumptions and some "smart" approaches in terms of data evaluation.

2.1 Missing information and general assumptions

The main challenge for this work is the missing engine thrust model, which is directly related to the aircraft's flight performance in daily operations. The engine efficiency directly corresponds to the fuel consumption which is a main driver for aircraft optimization to save fuel, reduce emissions and costs, and extend the aircraft range. Therefore, with the main modification of the Airbus A320neo being the new optimized engines, the first task for this work is to extract the engine thrust information from the recorded operational flight data.

Together with the reliable information about engine thrust, a very good prediction of aerodynamics is essential for a high quality flight performance model. Unfortunately, a detailed aerodynamic model of the Airbus A320neo or any other corresponding a-priori information was not available. Consequently, the aerodynamics must be determined from the recorded flight data. An initial guess for the aerodynamic model is derived from an existing simulation model of an Airbus A320-232, the DLR research aircraft "ATRA" (Advanced Technology Research Aircraft). The Airbus A320neo has some modifications and enhancements, but is basically well comparable to the previous versions of the Airbus A320 e.g., in terms of overall dimensions, or the size and aerodynamic performance of the empennage. Therefore, it is assumed that the a priori information on aerodynamic model structure and parameters is already sufficient for an initial representation of the A320neo aerodynamics and only needs some specific modifications.

Nevertheless, the change of thrust model formulation between the A320neo and the A320 ATRA will cause some changes in the drag model coefficients, mainly because of the integrated way of model determination: thrust and drag are directly correlated in flight and with a new engine thrust model, the drag coefficient model parameters must be adapted to guarantee the "measured" force equilibrium.

To do so, the main assumption for this work is that big data allows to decorrelate drag and thrust if the aerodynamics do vary due to high lift configuration changes and engine thrust is not dependent on these changes. It means that similar engine thrust conditions do exist for different aircraft configurations and consequently its drag, which than allows to determine each part individually. Moreover, using this assumption, it is not only possible to estimate aircraft drag and thrust, but also get unbiased values for both in terms of nearly correct zero lift drag and engine idle thrust.

2.2 Data evaluation process

For the determination of the Airbus A320neo flight performance from operational flight data a dedicated process was developed which aims to reduce both data size and computational effort. First, a flight data preprocessing allows to select only the information required for the further flight performance analysis and already makes all required computations before starting any further processing (loop). Second, the data are processed and analyzed based on specific engineering knowledge which does not require any artificial intelligence or highly complex evaluation methods. The process does contain of state-of-the-art data processing and system-identification techniques and is mainly based on aerospace engineering knowledge. This has the advantage, that the resulting models can be directly evaluated by analyzing the corresponding parameters (e.g. aerodynamic derivatives) and model outputs (e.g. engine thrust).

Figure 1 gives an illustration of the data evaluation process used for this work. This process contains five individual blocks necessary to process and analyze the data and to determine the desired models:

(a) Flight data processing: processing of the flight data by e.g., performing unit conversions, transformation of all relevant measurements to aircraft CG, determination of the aircraft configuration, anti-ice system status and flight condition, calculation of the atmospheric parameters using the international standard atmosphere.
(b) Aerodynamics evaluation: calculation of aerodynamics with a given model and from flight data depending on

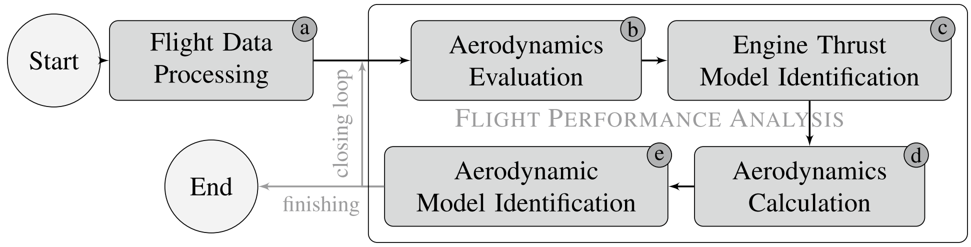

Fig. 1 Basic scheme of evaluation process used for the flight performance determination (aerodynamic model and thrust model identification)

available thrust information with simplified or complete equations.

(c) Engine thrust model identification: extraction of relevant data for thrust model identification, calculation of required thrust for the thrust model parameter estimation, engine thrust prediction in relation to the given flight data measurements with the identified model.
(d) Aerodynamics calculation: calculation of aerodynamic coefficients based on flight data and predicted engine thrust as reference for the aerodynamic model update.
(e) Aerodynamic model identification: new estimation of aerodynamic model parameters for all different aircraft configurations using system identification techniques.

For a specific information on the engine thrust model determination, the reader is referred to Refs. [12, 13].

After a successful aerodynamic model identification, the loop must be closed (at least for one single iteration) in order to newly determine the required engine thrust from measurements and predicted aerodynamics. This allows adjusting the aerodynamics and engine thrust to obtain the best force equilibrium for each data point. For this work, the loop is closed once and the “Flight Performance Analysis” in Fig. 1 is done two times until the evaluation is stopped.

The data evaluation and flight performance model determination process is coded in MATLAB®without any further distinct code optimization or parallelization. It is performed with MATLAB®2012b (64 bit) on a state of the art desktop computer (3.4 GHz multi-core processor, 64 GB memory).

3 Flight data base

This work is based on flight data recorded during operational flights on the pilots’ electronic flight bags (EFBs). A DLR-developed recorder was installed on the EFBs and used with different Airbus A320neo aircraft of a major European airline in preparation of the SESAR Very Large Demonstration (VLD2) ALBATROSS project. The recorder logs different ARINC messages using different interfaces depending on the EFBs it is installed on.

The flight data base is limited to reasonable airspeeds and altitudes sufficiently high above ground to guarantee the aircraft flying outside of the ground effect. Therefore, the following initial limits are used for the evaluation presented herein: height above ground above 50 ft and barometric altitude above 500 ft as well as true airspeed above 130 kts. These limits do not restrict the evaluation results, but allow to circumvent any special conditions of flight within ground effect. A brief overview of the flight data base as a result of the data pre-processing is given in Table 1. The number of data points does only include the data which was used for the evaluation and is therefore less than the total size of all data. Figure 2 visualizes the distribution of available flight data on an altitude-Mach plane split into the different aircraft flap/slat configurations.

The flight data sets used for the flight performance model determination are reduced to the relevant information. Initially, the data was recorded directly from aircraft buses/data streams and had to be processed in order to contain individual data channels with a sampling rate of 50 Hz. For each flight, the data sets finally contain: time stamp; body-fixed accelerations; angular rates; angle of attack, (estimated) angle of sideslip, true airspeed, Mach number, static air temperature; barometric (corrected) altitude, GPS altitude, radio height; engine fan speeds; aircraft gross weight, longitudinal CG position; landing gear status, flap and slat position; spoiler deflection (left/right, spoilers 2–5) and horizontal stabilizer deflection; wing and engine anti-ice system status.

There is one restriction with the available data sets: the records do not contain any information about the elevator deflection. It does only slightly affect the aircraft flight performance by a minor change of the overall aircraft lift, but is necessary to correctly predict the flight dynamics. But, with elevators only deflected during a short time during flight with the Airbus A320, it can be considered as an additional uncertainty within the overall process and is mainly relevant for the aerodynamics prediction outside the work presented herein.

The flight data are adequately preprocessed for aerodynamics evaluation and flight performance model determination (block (a) in Fig. 1). All data are converted to SI units and channels are corrected to comply with standard reference frames. Accelerations are transferred from the position of their measurement to the aircraft CG for further evaluation and aerodynamic coefficient calculation.

The evaluation of the resulting data takes around 1 h for the first cycle of thrust model prediction and aerodynamic

Table 1 Brief overview of flight data base used for evaluation

Number of aircraft		3
Number of flights		844
Number of data points		55,479,606
Data envelope	Min	Max
Baro altitude	500 ft	20 964 ft
Mach	0.1866	0.7311
Weight	48.57 t	73.44 t
Flap/slat configuration		Data points
FLAP 0		43,056,406
FLAP 1		1,914,563
FLAP 1+F		1,547,312
FLAP 2		4,514,991
FLAP 3		1,069,383
FLAP FULL		3,376,951

model parameters estimation and around 1 h 45 min for the whole closed loop. Note that the major part of the cycle is data handling, clustering and processing as well as the engine model determination.

4 Aircraft aerodynamics

The aircraft aerodynamics are the essential part of the flight performance. During the evaluation process, the aerodynamic model is used for evaluation and identification in block (b) and block (e) in Fig. 1. For this work, only lift and drag are required as these determine the aircraft flight performance. Hence, the aerodynamic model formulation given below is restricted to these two forces. Nevertheless, the data base would also allow to fundamentally predict aerodynamic moments and side force, if required, due to a large variety of flight conditions and maneuvers as well as a sufficient data quality.

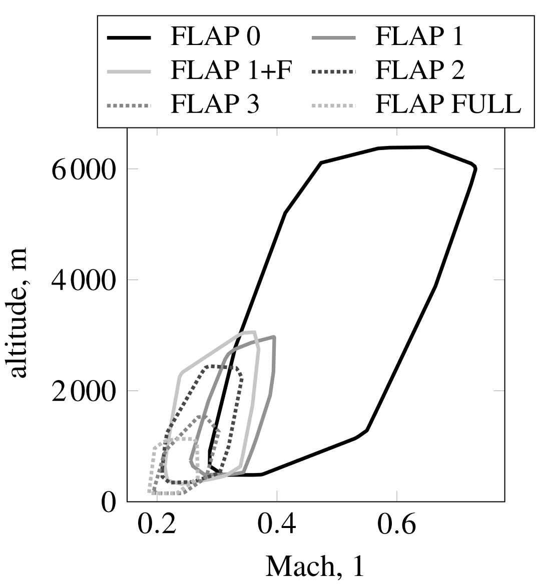

Fig. 2 Flight data envelope: altitude-Mach diagram for all flap/slat configurations

The herein used Airbus A320 aerodynamic model is formulated as a two-point model, splitting wing/body and horizontal tailplane influences ([14], see Fig. 3). For the wing/body aerodynamics, a nonlinear lift curve is considered, which allows to simulate flow separation effects [15]. The rigid body aerodynamic model is based on the well established derivative model formulation mainly used in DLR for system identification purposes. For example, a version of this formulation was used to model the aerodynamics of the former DLR in-flight simulator ATTAS (VFW 614), which is given in [16] as a result of the system identification process. The lift coefficient C_L is given by the two-point model consisting of the wing/body and the tailplane components:

$$C_L = C_{L,\mathrm{WB}} + C_{L,\mathrm{HT}} \cdot \frac{S_{\mathrm{HT}}}{S_{\mathrm{Wing}}} \cdot \cos(\alpha_{\mathrm{dyn}} - \varepsilon_{\mathrm{HT}}). \tag{1}$$

Due to the fact that only flight conditions above a certain altitude and height-above-ground are considered, the ground-effect can be neglected in the following equations. Hence, the wing/body contribution to lift is formulated as:

$$\begin{aligned} C_{L,\mathrm{WB}} = {} & C_{L0} + C_{L\alpha,\mathrm{WB}} \cdot \frac{1}{4} \cdot \left(1 + \sqrt{\widehat{X}_0}\right)^2 \cdot \alpha \\ & + C_{L,\mathrm{SP}} + C_{L,\mathrm{LG}} \cdot \delta_{\mathrm{LG}} + \Delta C_L(q, \xi, \dots) \end{aligned} \tag{2}$$

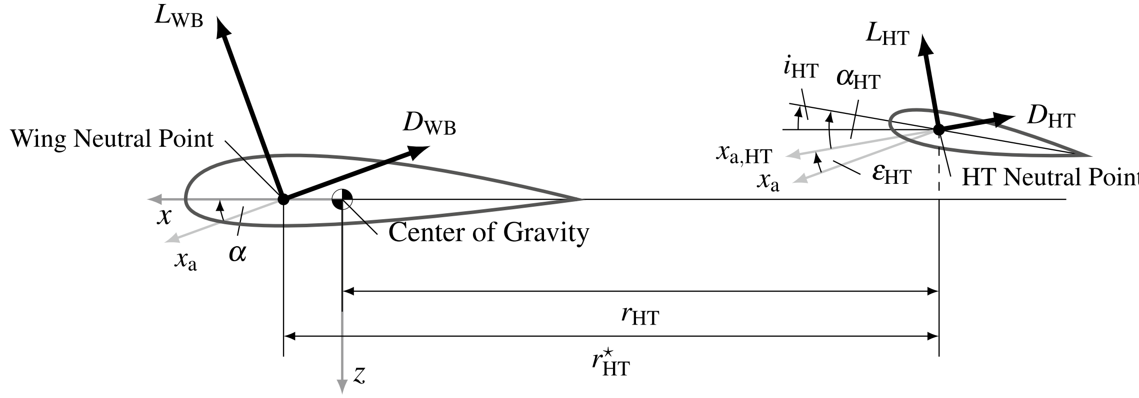

Fig. 3 Wing and horizontal tail geometry for the two-point model formulation, adapted from [14]

with $\Delta C_L(q, \xi, \dots)$ including additional contributions on the aircraft's lift coefficient due to e.g. dynamic effects and control surface deflections, which are not subject to the following analysis.

The non-dimensional location of the wing flow separation point $\hat{X}_0$ without hysteresis effects is defined by (see [17])

$$\hat{X}_0 = \frac{1}{2}\left(1 - \tanh\left(c_1 \cdot (\alpha - \alpha^{\star})\right)\right). \tag{3}$$

The effects of spoilers/airbrakes on the lift coefficient are considered by a combination of the influences of spoilers 2 and 3 and 4 and 5. Note, that the inner spoiler 1 is only used on ground for which reason it is not considered in the model formulation for the A320 in flight.

$$\begin{aligned} C_{L,\mathrm{SP}} = C_{L\alpha,\mathrm{SP}} \cdot \left(\sum_{i=2}^{5} \frac{\delta_{\mathrm{SP,RH},i} + \delta_{\mathrm{SP,LH},i}}{2}\right) \cdot \alpha \\ + C_{L,\mathrm{SP},23} \cdot \left(\sum_{i=2}^{3} \frac{\delta_{\mathrm{SP,RH},i} + \delta_{\mathrm{SP,LH},i}}{2}\right) \\ + C_{L,\mathrm{SP},45} \cdot \left(\sum_{i=4}^{5} \frac{\delta_{\mathrm{SP,RH},i} + \delta_{\mathrm{SP,LH},i}}{2}\right). \end{aligned} \tag{4}$$

The horizontal tailplane lift contribution $C_{L,\mathrm{HT}}$ (without ground effect) is formulated as:

$$C_{L,\mathrm{HT}} = C_{L0,\mathrm{HT}} + C_{L\alpha,\mathrm{HT}} \cdot \alpha_{\mathrm{HT}} + \Delta C_{L,\mathrm{HT}}(\eta, \dots) \tag{5}$$

with $\Delta C_{L,\mathrm{HT}}(\eta, \dots)$ including additional effects by e.g., the elevator deflection, which is not available in the flight data sets. The angle of attack at the tailplane α_{HT} is given by

$$\alpha_{\mathrm{HT}} = \alpha + \alpha_{\mathrm{dyn}} + i_{\mathrm{HT}} - \varepsilon_{\mathrm{HT}} \tag{6}$$

and the averaged downwash angle $\varepsilon_{\mathrm{HT}}$ at the tailplane's 25% chord line (without consideration of ground effect or wing flow separation) is

$$\varepsilon_{\mathrm{HT}} = \frac{\partial \varepsilon_{\mathrm{HT}}}{\partial \alpha} \cdot \left(\frac{C_{L0}}{C_{L\alpha,\mathrm{WB}}} + \alpha(t - \Delta t)\right). \tag{7}$$

The time delay Δt defines the run-time effects between wing and horizontal tailplane and is given by

$$\Delta t = \frac{r^{\star}_{\mathrm{HT}}}{V_{\mathrm{TAS}}}. \tag{8}$$

The dynamic angle of attack (due to a pitching motion) results from

$$\alpha_{\mathrm{dyn}} = \arctan\left(\frac{q \cdot r_{\mathrm{HT}}}{V_{\mathrm{TAS}}}\right). \tag{9}$$

The drag coefficient C_D is mainly driven by a quadratic drag polar formulation and extended by additional linear parts to cover influences from e.g., airbrakes, ailerons or wing flow separation. Note that the tailplane influences on the complete aircraft drag are covered due to the consideration of the whole aircraft lift coefficient C_L in the drag polar equation. Furthermore, an additional part of the drag equation covers the force depending on the turn of the horizontal tail lift around the local angle of attack α_{HT} acting in direction of the wing/body drag.

$$\begin{aligned} C_D = C_{D0} + k_1 \cdot C_L + \frac{C_L^2}{e \cdot \pi \cdot \Lambda} + C_{D,\mathrm{SP}} \\ + \frac{\partial C_D}{\partial \hat{X}}\left(1 - \hat{X}_0\right) + C_{D,\mathrm{LG}} \cdot \delta_{\mathrm{LG}} \\ - C_{L,\mathrm{HT}} \cdot \frac{S_{\mathrm{HT}}}{S_{\mathrm{Wing}}} \cdot \sin(\alpha_{\mathrm{dyn}} - \varepsilon_{\mathrm{HT}}) \\ + \Delta C_D(\beta, \xi, \dots) \end{aligned} \tag{10}$$

The effects of spoilers/airbrakes on the drag coefficient are again considered by a combination of the influences of spoilers 2 and 3 together with 4 and 5:

$$C_{D,\mathrm{SP}} = C_{D,\mathrm{SP},23} \cdot \left(\sum_{i=2}^{3} \frac{\delta_{\mathrm{SP,RH},i} + \delta_{\mathrm{SP,LH},i}}{2} \right) + C_{D,\mathrm{SP},45} \cdot \left(\sum_{i=4}^{5} \frac{\delta_{\mathrm{SP,RH},i} + \delta_{\mathrm{SP,LH},i}}{2} \right). \tag{11}$$

Note that different model coefficients are corrected for Mach number effects within the given large envelope using a Prandtl–Glauert correction.

The measured flight data allows to calculate directly the (translational) aerodynamic coefficients using the predicted engine thrust as given e.g., in Ref. [18]. Model coefficients and aerodynamic coefficients calculated from flight data (block (d) in Fig. 1) will then be the base for the equation-error parameter identification for the aerodynamic model update in Sect. 6 (block (e) in Fig. 1). The translational aerodynamic coefficients are given by

$$\begin{aligned} C_{X,\mathrm{M}} &= (m_{\mathrm{AC}} \cdot a_{x,\mathrm{CG}} - T_{\mathrm{x}})/(\overline{q} \cdot S_{\mathrm{Wing}}),\\ C_{Y,\mathrm{M}} &= (m_{\mathrm{AC}} \cdot a_{y,\mathrm{CG}} - T_{\mathrm{y}})/(\overline{q} \cdot S_{\mathrm{Wing}}),\\ C_{Z,\mathrm{M}} &= (m_{\mathrm{AC}} \cdot a_{z,\mathrm{CG}} - T_{\mathrm{z}})/(\overline{q} \cdot S_{\mathrm{Wing}}). \end{aligned} \tag{12}$$

The lift and drag coefficients result from the rotation of these coefficients around the angle of attack and angle of side-slip into the aerodynamic frame

$$\begin{aligned} C_{D,\mathrm{M}} &= -\big(C_{X,\mathrm{M}} \cdot \cos(\alpha) \cdot \cos(\beta) + C_{Y,\mathrm{M}} \cdot \sin(\beta) \\ &\qquad + C_{Z,\mathrm{M}} \cdot \sin(\alpha) \cdot \cos(\beta)\big),\\ C_{L,\mathrm{M}} &= C_{X,\mathrm{M}} \cdot \sin(\alpha) - C_{Z,\mathrm{M}} \cdot \cos(\alpha) \end{aligned} \tag{13}$$

Note that coefficients of the aerodynamic moments could not be calculated from the flight data, because no information about the aircraft's moments of inertia were available in the flight data which are essential for the calculation of the aerodynamic moments. To complete the aerodynamics model, if required, lateral aerodynamics as well as information for the pitching moment can be taken for this application from the initial model guess derived from the available DLR Airbus A320 ATRA model.

5 Engine thrust model

Engine thrust prediction is essential for any flight performance evaluation. Therefore, an engine thrust model development is part of the process described herein (see block (c) in Fig. 1), because there was no a-priori information about the engine thrust of the Pratt & Whitney "PW1100G" installed on the Airbus A320neo available for this work.

The thrust of a jet engine is dependent on several engine states and external parameters. Hence, the model formulation must cover the main influences to reliably predict the

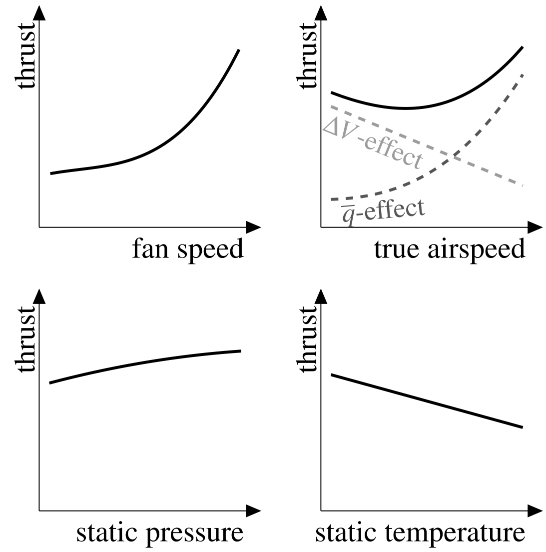

Fig. 4 General influence of different engine/aircraft states and atmospheric parameters on jet engine thrust, according to Refs. [19, 20]

engine thrust within the required flight envelope and for all relevant thrust settings. The general influence of different parameters on thrust are shown in Fig. 4. It is clearly visible that the jet engine thrust has a complex nonlinear behavior with the variation of the individual parameters. In consequence, the main regressors for the engine thrust model used in this work are defined as follows:

- engine fan speed,
- Mach number,
- barometric altitude,
- temperature offset.

Figure 5 gives an example on the evaluation of the predicted thrust model table for specific conditions. For a deeper insight in the nonlinear thrust table model determination, its definition and estimation as well as further information on the model quality, the reader is referred to Refs. [12, 13].

6 Aerodynamic model update

The initial aerodynamic model is updated considering the predicted engine thrust and given measurements (see block (e) in Fig. 1). Using the equations given in e.g., Ref. [18] and thrust information an aerodynamics data base with calculated lift and drag coefficients becomes available (see block (d) in Fig. 1). For aerodynamic model parameter estimation (see Sect. 4), an equation-error problem is formulated and solved with a Gauss–Newton algorithm [21].

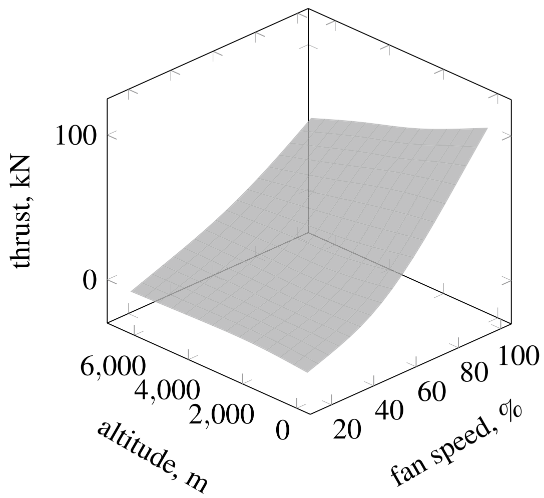

Fig. 5 Nonlinear thrust table evaluation at example conditions: variation of engine fan speed and altitude at $Ma = 0.4$; anti-ice off; from Ref. [12]

6.1 Aerodynamics model parameter estimation process

First, the focus is laid on the process development and validation. Therefore a model parameter update is only calculated for the FLAP 0 flap/slat configuration (clean aircraft). Although, the majority of available flight data consists of this flap/slat configuration which results in a large estimation problem the aerodynamic model update was initially expected to be marginal. In a future analysis, the aerodynamic model update process is extended for the remaining five flap/slat configurations. The aerodynamic parameters updated for FLAP 0 flap/slat configuration are:

- lift model: C_{L0}, $C_{L\alpha,\mathrm{WB}}$, $C_{L,\mathrm{SP},23}$, and $C_{L,\mathrm{SP},45}$,
- drag model: C_{D0}, k_1, e, $C_{D,\mathrm{SP},23}$, and $C_{D,\mathrm{SP},45}$.

The aerodynamic model in Sect. 4 consists of more parameters than the ones updated for this flap/slat configuration. On the one hand, some of these parameters are dynamic derivatives and therefore not relevant for a successful flight performance prediction. Also the flow separation formulation is mainly not relevant for this work, because the data base neither contain the corresponding information nor will the aircraft behavior be predicted at high angles of attack in the foreseen model application. But nevertheless, for e.g., FLAP FULL configuration it can be necessary to adapt some of the flow separation parameters to modify the lift curve in order to obtain slightly nonlinear characteristics at higher angles of attack which can be relevant even for normal flight conditions. Note, that the different high lift configurations will be considered as individual aerodynamic cases including their own parameter sets between which will be interpolated during configuration changes. On the other hand, there are some parameters which could be relevant for the aircraft's flight performance prediction, but cannot be estimated using the given data base. For example, the modification on the aircraft's wing changes the free flow behind the wing and consequently the downwash at the horizontal tail. The downwash effect related to the wing's lift[1] is included in the model formulation (see Eq. (7)), but cannot be identified from flight data due to a lack of information. Furthermore, horizontal tail aerodynamics like lift slope or elevator effectiveness are assumed to be well represented by the initial model. This is a simplification of the problem which is necessary, because these parameters cannot be estimated due to a lack of information in the data. In addition, horizontal tail aerodynamics should not need to be updated, because the modification of the Airbus A320neo is mainly related to wing and engines and not to the horizontal tail. Hence, the information available from the initial model guess based on DLR's Airbus A320 ATRA model will be used for the not-identifiable parameters, e.g., downwash in Eq. (7) or horizontal tail aerodynamics in Eq. (5). Including this, the model will be also able to predict more complex flight situations which is required for the implementation in LNAS and a correct flight performance prediction during the whole descent and approach.

The parameter estimation process in this case is driven by a deep knowledge about the preceeding successful aircraft model identification. The aerodynamic model does contain several parameters which are difficult to estimate but are required for a good flight performance prediction. Hence, a certain process must be applied to obtain the corresponding estimates. First, lift and drag parameter estimation is split. Although the equation-error method allows to estimate the lift and drag parameters together, a separation into two individual estimation problems avoided correlation effects between the model parameters. Reducing the whole optimization problem to smaller problems further allows finding an acceptable solution much easier. The whole estimation process for the aerodynamic model is mainly driven by the goal to solve a big data problem which is the objective of this work.

Within this estimation process, the least-square optimization problem to obtain the desired parameter estimates $\widehat{\boldsymbol{\theta}}$ is formulated as:

$$\widehat{\boldsymbol{\theta}} = \underset{\boldsymbol{\theta}}{\operatorname{argmin}} \left(\boldsymbol{\theta} \rightarrow \sum_{i=1}^{N} \left(z_i - \boldsymbol{y}_i(\boldsymbol{\theta}) \right)^2 \right), \tag{14}$$

[1] In case of the model formulation used herein this downwash effect is dependent on the delayed angle of attack considering the run time effect, which is linearly correlated with lift.

Table 2 Relative change of lift and drag model coefficients after model update; FLAP0 flap/slat configuration

Change of lift model parameters				
C_{L0}	$C_{L\alpha,\mathrm{WB}}$	$C_{L,\mathrm{SP},23}$	$C_{L,\mathrm{SP},45}$	
7.55%	−0.13%	124.72%	8.59%	
Change of drag model parameters				
C_{D0}	k_1	e	$C_{D,\mathrm{SP},23}$	$C_{D,\mathrm{SP},45}$
−5.23%	−60.03%	13.71%	−52.21%	−42.88%

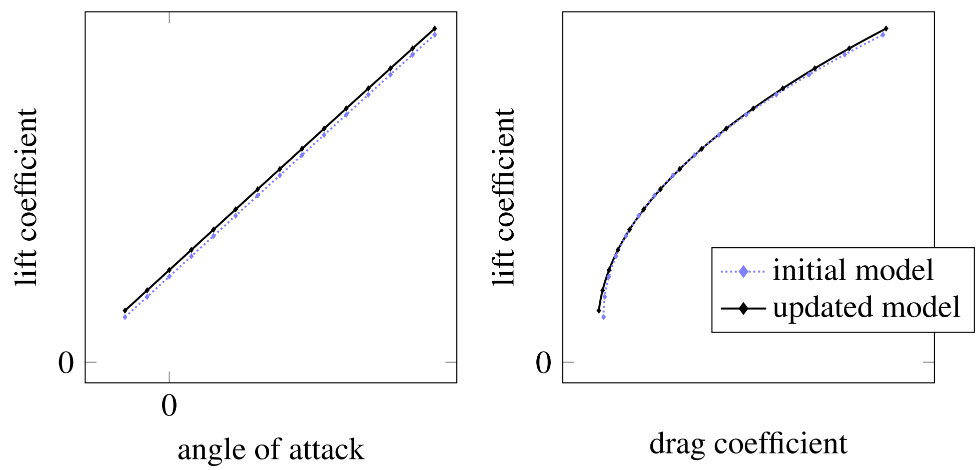

Fig. 6 Aerodynamic model evaluation: comparison of complete aircraft coefficients for updated model after parameter estimation (solid lines) and initial model (dashed lines); all high lift configurations and gear up, without control surface deflections and Mach number correction

where z_i describe the vector of the individual aerodynamic coefficients calculated from measured flight data and $\boldsymbol{y}_i$ the vector of the corresponding aerodynamic model output. The application of a Gauss–Newton algorithm allows to easily solve this problem.

6.2 Aerodynamic model parameter update

The updated aerodynamic model parameters are obtained by running the process loop in Fig. 1 for the given flight data. The relative change of parameter values between initial guess and updated model are given in Table 2. In general, the estimated parameter values show that the necessary changes were very small and the initial model guess was very good. The spoiler influence on lift was initially under-predicted, which is changed for the updated model. In case of drag, the spoiler influences seemed to be initially over-predicted which is corrected with the updated model results.

A visualization of the updated aerodynamic model is given in Fig. 6 for the lift curve and drag polar. The figure contains the model result plots within the regions of angle of attack and lift coefficient available in the flight data base. In addition, plots of the initial model are given for comparison. Note that the aerodynamic model evaluations to calculate the lift curve and drag polar do not contain Mach number corrections or control surfaces deflections. As given in Table 2, the updated model for the FLAP 0 configuration does not differ much from the initial guess. The minor changes represent aerodynamic lift performance better and sightly reduce the aircraft drag, which is reasonable because the initial model guess is related to an Airbus A320-232 and the updated model describes the enhanced Airbus A320neo. Note that the relative changes provided in Table 2 might be misleading due to their apparently large values, e.g., the linear drag polar shift k_1, although their influence on the model results are small. This is a results of already very small parameter values for the initial model guess. In contrast, for the spoiler influence, the correction is indeed significant.

Figures 7 and 8 show lift curves and drag polars, each for one individual example flight (FLAP0 configuration only) with the same aircraft. Note that these results can only be shown reasonably as lift curves and drag polar for individual flights. Plotting together more than one flight or for example all data available makes it almost impossible to visually extract any information and is therefore not reasonable. These figures show the proof of match between the updated model prediction and the data calculated from measurements using the already defined nonlinear engine thrust model as described in Sect. 5. In addition to the updated model prediction, the simulation results for the initial aerodynamic model are shown as well. Having the complete recorded data from a single flight, the influence of e.g., spoiler deflection on

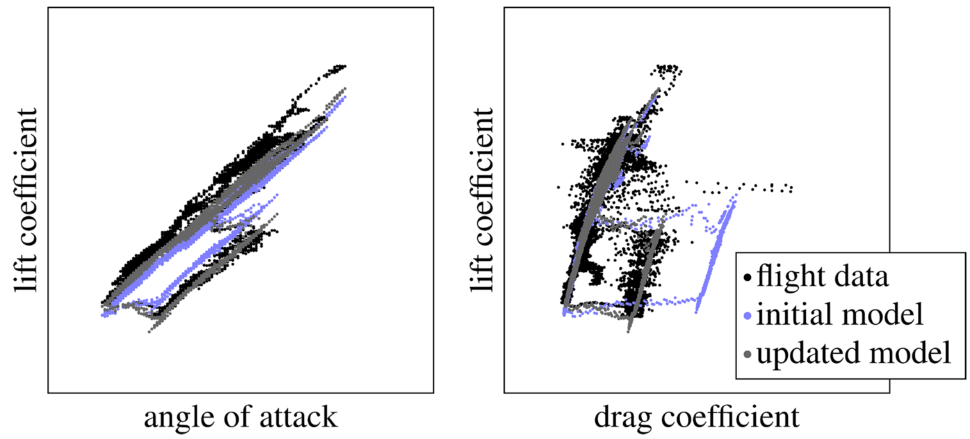

Fig. 7 Aerodynamic model proof of match: example of operational flight data from one specific flight; comparison of lift and drag coefficients calculated from flight data measurements, initial and updated aerodynamic model; example flight 1

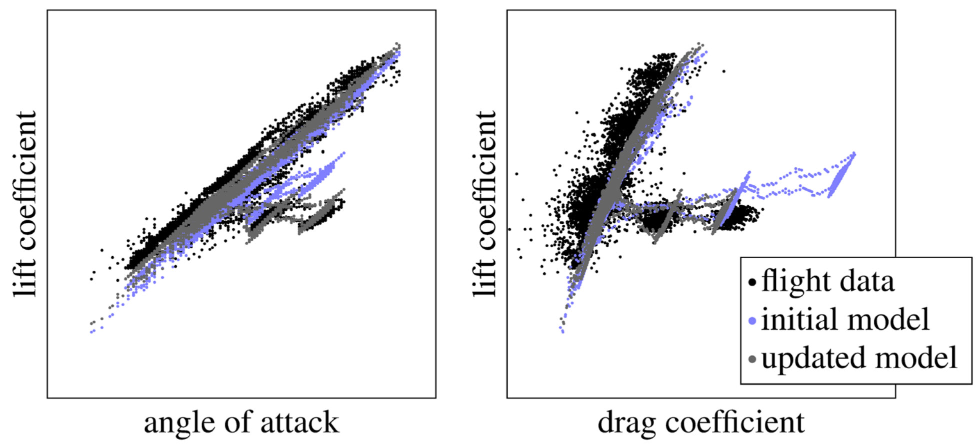

Fig. 8 Aerodynamic model proof of match: example of operational flight data from one specific flight; comparison of lift and drag coefficients calculated from flight data measurements, initial and updated aerodynamic model; example flight 2

aerodynamics becomes visible. With the spoilers deflected, the lift curve is shifted down, because the lift is reduced. In parallel, the drag polar is shifted to the right depending on the magnitude of the spoiler deflection, because the drag is significantly increased as desired. The two examples show that the initial model underestimates the spoiler influence on lift and overestimates the corresponding influence on drag in parallel. Hence, the updated model with the adapted parameters in Table 2 allows to match the given data much better. Similar results are obtained from the other flights in the data base which are not shown herein.

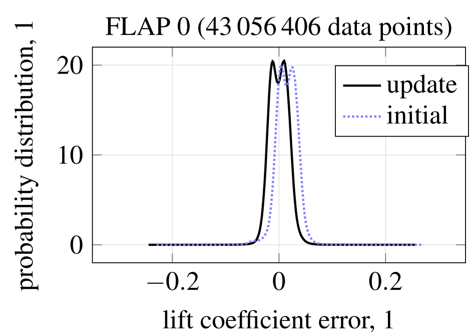

Fig. 9 Probability distribution of lift coefficient residuals; initial and updated aerodynamics

6.3 Statistical analysis

The aerodynamic model results are evaluated according to the model's ability to predict the aerodynamic coefficients directly calculated from measurements by the application of statistical analysis methods. Figures 9 and 10 contain the probability distributions of the lift and drag coefficient residuals with the updated and the initial aerodynamic model, each based on a histogram with 300 bins. In general, it gets clearly visible that the updated model is able to predict the measurements much better than the initial model guess.

Figure 9 shows that the lift coefficient residuals are centered around zero with a very narrow bimodal distribution.

The following four mathematical moments are used for this statistical analysis in order to further reveal their ability to well predict the measurements:

(1) mean value: expected value of residuals; for good model match it must be near zero;

Table 3 Mathematical moments of probability distribution of lift and drag coefficient residuals; comparison of updated and initial model results

Lift model	Mean value	Standard deviation	Skewness	Kurtosis
Updated	$2.797 \cdot 10^{-4}$	$1.7460 \cdot 10^{-2}$	0.1020	3.55
Initial	0.0149	$1.9072 \cdot 10^{-2}$	−0.3710	4.63
Drag model				
Updated	$4.328 \cdot 10^{-5}$	$1.7987 \cdot 10^{-3}$	0.7529	12.65
Initial	$2.490 \cdot 10^{-4}$	$2.8113 \cdot 10^{-3}$	−2.7816	19.81

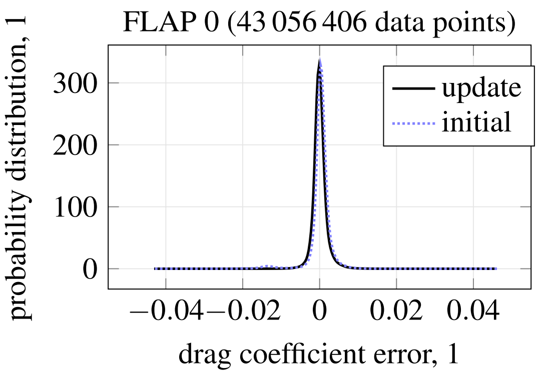

Fig. 10 Probability distribution of drag coefficient residuals; initial and updated aerodynamics

(2) standard deviation: variation of error between measurement and prediction; small values indicate very good predictions, large values point out that the model is not able to match the measurements well;
(3) skewness: measure of asymmetry of the probability distribution in relation to its mean; negative values indicate longer left tail, positive values a longer right tail and zero values are obtained for balanced distributions;
(4) kurtosis: "peakness" of the probability distribution, higher values correspond to a large peak around the mean; for interpretation of the kurtosis, it is often compared to the value 3 of the normal distribution leading to the "excess".

The corresponding mathematical moments are given in Table 3. These values underpin the visual interpretation of Fig. 9. Mean value and standard deviation show that the updated model better predicts the aircraft's lift coefficient calculated from the flight data sets. The further evaluation of the shape of the different residual distributions by skewness and kurtosis show that the shape could only be enhanced in the way of better symmetry (smaller skewness).

Figure 10 shows the probability distribution of drag coefficient residuals—also based on a histogram with 300 bins—with a very small variation for initial and updated model. Nevertheless, the updated model has a more uniform residual distribution and is able to well predict aircraft's drag. These results are again underpinned by the mathematical moments given in Table 3. Mean value and standard deviation are significantly reduced by the updated model which directly indicated is quality and ability to predict the aircraft's drag coefficient obtained from flight data. The distribution's shape could be enhanced in the way of better symmetry (smaller skewness).

7 Conclusion

This paper describes the development of a flight performance model for the Airbus A320neo from operational flight data. The novel developed process combines the identification of aircraft aerodynamics together with the definition of an engine thrust model. It faces the challenges of the aerodynamic parameter estimation together with the directly linked engine thrust by solving the big data problem given through the large amount of flight data: it is solved by application of a smart data approach utilizing fundamental flight mechanics knowledge and system-identification techniques. The resulting flight performance model structure provides several advantages for usage in aircraft simulation tasks compared to models developed with e.g. different deep learning methods used in big data science.

The work presented contains the first results for the aerodynamic model parameter updates. Based on the available flight data sets and the previously identified engine thrust model structure, the new results for one specific flap/slat configuration (FLAP 0) show that the updated model is evidently better able to describe the aircraft aerodynamics than the initial model guess based on an a-priori Airbus A320 simulation model.

In a future work, the presented approach will be used for updating the aerodynamic model for all remaining five flap/slat configurations and provide a similar statistical evaluation of results as given herein. Finally, the models for engine thrust and aerodynamics will be implemented in an aircraft simulation model for the Airbus A320neo and validated with the flight data sets.

Acknowledgements The author wants to specially thank his colleague Nicolas Fezans for his contributions to this work through several fruitful discussions. Part of this work is related to the SESAR Very Large Demonstration (VLD2) ALBATROSS project: the most energy-efficient flying bird; this project has received funding from the SESAR Joint Undertaking under the European Union's Horizon 2020 research and innovation programme under grant agreement No 101017678.

Funding Open Access funding enabled and organized by Projekt DEAL.

Declarations

Conflict of interest The author has no competing interests to declare that are relevant to the content of this article.

References

1. European Commission.: Flightpath 2050 Europe's Vision for Aviation. Katalog KI-31-11-098-EN-C. European Union, Luxemburg (2011). https://doi.org/10.2777/50266
2. Georg Kühne, C., Scholz, M., Abdelmoula, F.: LNAS—a pilot assistance system for energy-optimal approaches using existing aircraft-infrastructure. In: Advanced Aircraft Efficiency in a Global Air Transport System Conference (AEGATS). AEGATS 2018, Toulouse, France, October 23–25, 2018. Association Aéronautique et Astronautique de France (3AF) (2018)
3. Abdelmoula, F., Scholz, M.: LNAS—a pilot assistance system for low-noise approaches with minimal fuel consumption. In: 31st ICAS Congress, Belo Horizonte, Brazil, September 9–14, 2018. International Council of the Aeronautical Sciences (ICAS) (2018)
4. Ghazi, G., Botez, R.M.: Identification and validation of an engine performance database model for the flight management system. J. Aerosp. Inf. Syst. **16**(8), 307–326 (2019). https://doi.org/10.2514/1.I010663
5. Simmons, B.M.: System identification for propellers at high incidence angles. In: AIAA SciTech Forum, number AIAA 2021-1190, Virtual Event, January 11–15 and 19–21, 2021. American Institute of Aeronautics and Astronautics, Inc. (AIAA) (2021). https://doi.org/10.2514/6.2021-1190
6. Deiler, C.: Evaluation of aircraft performance variation during daily flight operations. In: German Aerospace Congress, Deutsche Gesellschaft fur Luft- und Raumfahrt (DGLR), Friedrichshafen, Germany, September (2018). https://doi.org/10.25967/480025
7. Deiler, C., Fezans, N.: Performance-based ice detection methodology. J. Aircraft **57**(2), 209–223 (2020). https://doi.org/10.2514/1.C034828
8. Krajček, K., Nikolić, D., Domitrović, A.: Aircraft performance monitoring from flight data. Techn. Gazette **22**(5), 1337–1344 (2015). https://doi.org/10.17559/TV-20131220145918
9. Deo, V.A., Silvestre, F., Morales, M.: Flight performance monitoring with optimal filtering applications. Aeronaut. J. **124**(1272), 170–188 (2020). https://doi.org/10.1017/aer.2019.142
10. Ghazi, G., Gerardin, B., Gelhaye, M., Botez, R.M.: New adaptive algorithm development for monitoring aircraft performance and improving flight management system predictions. J. Aerosp. Inf. Syst. **17**(2), 97–112 (2020). https://doi.org/10.2514/1.I010748
11. Ghazi, G., Botez, R.M., Domanti, S.: New methodology for aircraft performance model identification for flight management system applications. J. Aerosp. Inf. Syst. **17**(6), 294–310 (2020). https://doi.org/10.2514/1.I010791
12. Deiler, C.: Engine thrust model determination from large operational flight data base. In: 6th CEAS Conference on Guidance, Navigation and Control (EuroGNC), Berlin, Germany, 3–5 May, 2022. Council of European Aerospace Societies (CEAS) (2022)
13. Deiler, C.: Engine thrust model determination and analysis using a large operational flight database. CEAS Aeronaut. J. **14**(1), 29–45 (2023). https://doi.org/10.1007/s13272-022-00625-y
14. Moennich, W.: Ein 2-punkt-aerodynamikmodell für die identifizierung. In: Symposium 'Systemidentifizierung in der Fahrzeugdynamik', Paper No 3.1 in DFVLR Mitteilung, 87-22 (1987) (in German)
15. Fischenberg, D., Jategaonkar, R.V.: Identification of aircraft stall behavior from flight test data. In: RTO Systems Concepts and Integration Panel (SCI) Symposium, number 17, Madrid, Spain, May 5–7, 1998. NATO Research and Technology Organisation (1998)
16. Jategaonkar, R.: ldentification of the Aerodynamic Model of the DLR Research Aircraft ATTAS from Flight Test Data. DLR-FB 90-40. Deutsche Forschungsanstalt für Luft- und Raumfahrt e. V. (DLR), Cologne, Germany (1990)
17. Fischenberg, D.: Identification of an unsteady aerodynamic stall model from flight test data. In: AIAA Atmospheric Flight Mechanics Conference, Baltimore, Maryland, USA, number AIAA 95-3438-CP, pp. 138–146, August 7–10, 1995. American Institute of Aeronautics and Astronautics, Inc. (AIAA) (1995). https://doi.org/10.2514/6.1995-3438
18. Raab, C.: Rapid aerodynamic parameter identification on a large transport aircraft. In: AIAA Atmospheric Flight Mechanics Conference at SciTech. National Harbor, Maryland, USA, January 2014. American Institute of Aeronautics and Astronautics, Inc. https://doi.org/10.2514/6.2014-0730 (2014)
19. Irwin, E.: Traeger, 3rd edn. Aircraft Gas Turbine Engine Technology, Glencoe/McGraw-Hill, Westerville, OH, USA (1996)
20. Nicolai, L.M., Carichner, G.E.: Fundamentals of Aircraft and Airship Design, vol. 1—Aircraft Design. American Institute of Aeronautics and Astronautics, Inc. (AIAA), Reston, Virginia, USA (2010). https://doi.org/10.2514/4.867538
21. Jategaonkar, R.V.: Flight Vehicle System Identification—A Time Domain Methodology. Progress in Astronautics and Aeronautics, vol. 245, 2nd edn. American Institute of Aeronautics and Astronautics, Inc., Reston (2015)